Cross-flow filtration for the recovery of lipids from microalgae aqueous extracts: membrane selection and performances

Erika Clavijo Rivera, Liliana Villafaña-López, Shuli Liu, R Vinoth Kumar, Michèle Viau, Patrick Bourseau, Cécile Monteux, Matthieu Frappart, Estelle Couallier

▶ **To cite this version:**

Erika Clavijo Rivera, Liliana Villafaña-López, Shuli Liu, R Vinoth Kumar, Michèle Viau, et al.. Cross-flow filtration for the recovery of lipids from microalgae aqueous extracts: membrane selection and performances. Process Biochemistry, 2020, 89, pp.199-207. 10.1016/j.procbio.2019.10.016 . hal-02319838

HAL Id: hal-02319838
https://hal.science/hal-02319838

Submitted on 18 Oct 2019

HAL is a multi-disciplinary open access archive for the deposit and dissemination of scientific research documents, whether they are published or not. The documents may come from teaching and research institutions in France or abroad, or from public or private research centers.

L'archive ouverte pluridisciplinaire **HAL**, est destinée au dépôt et à la diffusion de documents scientifiques de niveau recherche, publiés ou non, émanant des établissements d'enseignement et de recherche français ou étrangers, des laboratoires publics ou privés.

Cross-flow filtration for the recovery of lipids from microalgae aqueous extracts: membrane selection and performances

Erika Clavijo Rivera[a], Liliana Villafaña-López[a,b], Shuli Liu[a,c], R. Vinoth Kumar[a,d], Michèle Viau[d], Patrick Bourseau[a,e], Cécile Monteux[f], Matthieu Frappart[a], Estelle Couallier[a,*]

[a] *CNRS, GEPEA, Université de Nantes, 37 Boulevard de l'université, BP 406, 44602 Saint-Nazaire cedex, France*
[b] *CIATEC A.C., Centro de Innovación Aplicada en Tecnologías Competitivas, Omega 201, Col. Industrial Delta, 37545 León, Gto., Mexico.*
[c] *ADEME, 20 avenue du Grésillé, BP90406, 49004 Angers cedex 01, France*
[d] *INRA, BIA, Rue de la Géraudière, BP 71627, 44 316 Nantes Cedex 3, France*
[e] *Université de Bretagne Sud, Rue de Saint-Maudé, BP 92116, 56321 Lorient Cedex, France*
[f] *CNRS, PPMD, SIMM, 10 rue Vauquelin, 75231 PARIS CEDEX 05, France*

Abstract

see below

Declaration of interest: none.

*Corresponding author
Email address: estelle.couallier@univ-nantes.fr (Estelle Couallier)

Abstract. The biorefinery of microalgae necessitates innovative choices of soft and energy-efficient processes to guarantee the integrity of fragile molecules and develop eco-friendly production. A wet processing of biomass is proposed, which avoids expensive drying steps. It includes harvesting, cell disruption, and fractionation of the target compounds. Membrane filtration is a promising clean fractionation step. In this paper, the recovery of lipids from starving *Parachlorella kessleri* aqueous extracts by cross-flow filtration was studied. A model solution was formulated to test four membranes of different materials (PVDF, PES, PAN) and cut-offs (200 kDa - 1.5 µm). The hydrophilic PAN 500 kDa membrane presented the best performance (flux stability, permeate flux, lipid retention, and cleanability) and was therfore selected for filtrating real aqueous extracts. Similar permeation fluxes were obtained with model and real products: 34 - 41 L h^{-1} m^{-2} respectively. The coalescence of lipid droplets was observed with model solutions but not with real products, less concentrated. The lipids from the real products were wholly retained by the PAN membrane, whereas some of the polysaccharides and proteins were able to permeate. An optimization of the coupling between culture, cell disruption, clarification, and filtration would allow a good concentration and purification of the lipids from microalgae.

Keywords. microalgae biorefining membrane filtration lipidsemulsion polyacrylonitrile membrane

1. Introduction

The biorefinery of renewable resources like microalgae offers great opportunities for substituting biomolecules (lipids, proteins, carbohydrates, and antioxidants) for traditional raw materials in various industry sectors, such as food/nutrition and animal feed, cosmetics, pharmacy, energy and green chemistry. Such strategies necessitate innovative choices of soft and energy-efficient processes to guarantee the integrity of fragile molecules and develop eco-friendly production. For large-scale production (food, energy and green chemistry), a wet processing of biomass is proposed, which avoids expensive drying steps and reduces solvent use [1–5]. However, the energetically efficient extraction of biomolecules at low cost on an industrial scale is not yet mature [6–11]. Wet biomass treatment includes 1- harvesting, 2- cell disruption step to release the valuable biochemicals in the aqueous phase, 3- fractionation steps (extraction, concentration and purification).

The integration of membrane processes into the downstream processing of the microalgae involves the harvesting and the concentration of microalgae [12–18], but membrane filtration is also a promising clean separation process for the fractionation steps [19–26].

In this work we focus on the recovery and concentration of lipids from *Parachlorella kessleri*, cultivated in starving conditions to enhance lipid production. Lipid recovery from microalgae has mainly been carried out with

supercritical CO_2 on dried matter or by solvent extraction [20; 27; 28]. In this study the membrane processes are developed. After grinding of the microalgae and centrifugation, the supernatant contains large quantities of the lipids, dispersed in water [29]. Clavijo Rivera et al. [29] demonstrated that after bead milling and centrifugation of *Parachlorella kessleri*, the supernatant contains emulsified lipids in the aqueous phase. This lipid phase contains neutral lipids (triglycerides and free fatty acids) and polar lipids (phospho and glycolipids). The purpose of this work is to study the recovery and concentration of these valuable compounds by membrane processes.

Membrane filtration has previously been used for the recovery of emulsified lipids in effluents from different industries (food, petroleum, metallurgy, etc.), mostly using micro or ultrafiltration membranes [30–32]. The lipids are mixed with surfactants which strongly influence the separation [33]. The lipids separation from the aqueous phase implies concentration of the lipids on the one hand, and/or destabilization of the water–oil interface to induce coalescence on the other. The concentration of the lipids into the retentate necessitates hydrophilic membranes to limit the fouling of the membrane by organic matter. These membranes can be made of cellulose, polyacrylonitrile (PAN), polyethersulfone (PES), hydrophilated polyvinylidene fluoride (PVDF) [34–38]. New hydrophilic membranes are also being developed [39–41]. Coalescence is enhanced with hydrophobic membranes (PVDF, polytetrafluoroethylene PTFE, polypropylene PP) [34; 35; 42].

However, the fractionation of disrupted microalgae has rarely been investigated [21–25; 43]. Prediction and control of the membrane filtration in complex mixtures with macromolecules, organic and mineral compounds, is known to be difficult.

Giorno et al. [43] studied triglyceride separation from a wet sonicated biomass. They used ultrafiltration cellulose membranes with 30 and 100 kDa molecular weight cutoffs and achieved water permeation flux between 22 and 27 L h^{-1} m^{-2} with a transmembrane pressure (TMP) of 0.14-0.2 bar for concentration experiments. Montalescot et al. [23] also studied the wet biomass fractionation after bead milling or high pressure disruption. The author used ceramic membranes with a porous diameter of between 50 nm and 1.4 µm. Unlike with Giorno, the lipid transmission was less than 4%. A strong retention of proteins and carbohydrates was also mentioned. Following centrifugation, the filtration of the supernatant allowed a better transmission of carbohydrates. Lorente et al. [25] compared cross-flow and dynamic filtration with a vibratory shear enhanced processing (VSEP) for the concentration of lipids from a steam-exploded biomass before solvent extraction. They tested several membranes and selected two: a PES 5 kDa and a PVDF 100 kDa. They used a transmembrane pressure equal to 5 bar and managed to concentrate the lipids with a permeate flux between 7 and 25 L h^{-1} m^{-2}. The authors recorded a strong reduction (50-60%) in the solvent volume needed for lipid extraction after filtration. Safi et al. [24] tested membrane filtration to recover proteins from disrupted cells. They compared high pressure

disruption (HPD) and enzymatic cell disruption combined with ultrafiltration and diafiltration. They tested PES membranes with different molecular weight cut offs (MWCO = 300, 500 and 1000 kDa). Strong fouling was noted for the largest MWCO. The best permeation flux was achieved with PES 300 kDa (30-40 L h^{-1} m^{-2}), at 2 bar. The best total protein recovery was obtained with enzymatic hydrolysis and ultrafiltration/diafiltration (24%) but the proteins were denatured, whereas the HPD led to lower protein recovery (17%) but the native structure seemed to be preserved.

The above authors encountered difficulties in fractionating of a complex medium coming from disrupted cells and membrane fouling. The composition of microalgae extracts depends on culture batches, grinding, clarification and storage conditions prior to filtration [29]. This variability in the characteristics of the filtration feed solution may lead to different interactions between molecules in the liquid phase and also with the membrane. Consequently, differences in the feed solution are expected to influence filtration performances and hinder the comparison of results for accurate selection of an adapted membrane, and operating conditions for the separation process. For this reason, it would be helpful to use mixtures with well–known characteristics.

In this work, a model solution was formulated, based on the analysis of the lipid fraction from *Parachlorella kessleri* aqueous extracts [29]. This solution was then filtered to evaluate the performances (retention, flux and cleanabil-

ity) of PAN, PES and PVDF membranes to concentrate lipids. The most appropriate material and conditions were then selected and verified on real microalgae fractions.

2. Material and methods

2.1. Parachlorella kessleri culture, harvesting and storage

The strain *Parachlorella kessleri* was cultivated in autotrophic conditions using a BBM medium. The first step was to inoculate the pre-culture in a bubble column photobioreactor (PBR) with 15 L of normal BBM medium (0.75 g L^{-1} $NaNO_3$). After 10 days, the culture reached a stationary growth phase and a modified BBM medium (0.23 gL^{-1} $NaNO_3$) was gradually added to reach 100L in nitrogen starvation conditions. The PBR was aerated with 0.5-1 L min^{-1} CO_2 and 5 L min^{-1} filtered air. The pH was maintained at 7.5 through pH-controlled addition of carbon dioxide to the airflow. During the starvation phase, the continuous white light intensity was 100-150 µmol m^{-2} s^{-1} and the culture temperature was between 22 to 25°C. The microalgae were harvested by centrifugation at 5400 *g* (ROUSSELET ROBATEL DRA320VX, France). A concentrated paste containing 1.5% to 2.0% dry matter was obtained and then stored frozen at -20°C before the cell disruption.

2.2. Biomass pretreatment

The frozen microalgae paste was thawed in the fridge at 4°C for one night and resuspended to 5 g L^{-1} with phosphate buffer (pH 7.4, Conductivity 790 µScm^{-1}) and stirred at room temperature. The dilution was chosen to perform two filtration experiments with the aqueous extract obtained from 100 L of the initial culture. The bead milling (Dyno-mill multi labo, Muttenz, WAB, Switzerland) was operated in pendulum mode [44; 45]. The flow rate was set at 150 mL min^{-1}. The filling ratio with the glass beads (average diameter 0.65 mm) was 75% and the impeller tip velocity was 8 m s^{-1}. The bead milling was combined with two plate heat exchangers for enzyme inactivation. The resuspended biomass was heated at 60°C with a plate heat exchanger before entering the bead mill, and cooled at the outlet to 5°C using a plate cooler. Three passes in the bead mill and one pass were carried out respectively for the first and second experiments. The disrupted cells were centrifuged at 12000 g, 5°C for 20min (SORVALL LYNX 6000, Thermo Scientific). The recovered supernatants SN_1 (first experiment) and SN_2 (second experiment) were stored at 4°C for subsequent filtrations.

2.3. Formulation of the model solution

The model solution was an oil-in-water emulsion representing the supernatant of a concentrated (x40) pre-treated culture, after bead milling and separation of the cell fragments by centrifugation. The emulsion granulometry, pH and conductivity were based on the characteristics of a real supernatant

[29]. It contained $2\%_w$ of lipids in an aqueous phase close to a fresh water culture medium, with a pH 7.4 and a conductivity equal to 790 µS cm^{-1}. The lipid phase contained $70\%_w$ of neutral lipids from a mixture of vegetable oils and $30\%_w$ of polar lipids comprising commercial products called A and B here.

2.3.1. Products selection

Based on the total fatty acid composition of a supernatant from a real microalgae extract (after grinding and centrifugation) [29], a mixture of vegetable oils was selected for formulation of the model solution. The amphiphilic compounds contained in real microalgae extracts are phospholipids (such as phosphatidylcholine PC and lysophosphatidylcholine LPC), glycolipids, and free fatty acids. Two commercial surfactants composed mainly of polar lipids were therfore chosen to stabilize the emulsion. One of the emulsifying products was selected to represent phospholipids (A). It contained $>96.2\%_w$ of PC, $<4\%_w$ of LPC, and $< 0.3\%_w$ of tocopherol. The other product (B) represented glycolipids and smaller aliphatic surfactants and contained fatty alcohols and alkylpolyglycosides.

2.3.2. Emulsification

A preliminary study was carried out to define the emulsification conditions and obtain a stable emulsion with the desired granulometry (0.5-5 μm). The process was performed using a high-speed dispersing unit, IKA Ultra-Turrax T 25 basic, with a dispersing tool 13 mm in diameter. The aqueous

phase (pH 7.4, 790 µScm^{-1}) was mixed with A (15%$_w$ of the total lipid content) at 80°C and the vegetable oils with B (15%w of the total lipid content) at 80°C. The aqueous and the oil phases were then mixed (28300 rpm, 30 min) and cooled to ambient temperature for 24h with gentle stirring at 700 rpm.

2.4. Membrane filtration

2.4.1. Selected membranes

Four organic membranes (Orelis Environment) were tested (table 1): one made of polyethersulfone (PES), a current polymer used for membrane filtration in the agrofood industry, one made of polyacrilonitrile (PAN) used in emulsion filtration, and two made of polyvinylidene fluoride (PVDF), useful for emulsion destabilization.

Before use, each new sheet of membrane (8.5x17.9 cm) was rinsed, cleaned and compacted until constant water flux was reached to ensure the stability of the membrane during filtration tests. Membrane compaction was performed as follows: water was circulated in the system in full recycling mode at room temperature. TMP was increased every 15 min from 0.25 bar to 1 bar in 0.25 bar steps. Pressure was kept constant until a stable permeate flux was achieved.

2.4.2. Filtration experimental set-up

The tests were performed in a crossflow filtration set-up (Rayflow 100, Rhodia, Orelis) with an effective membrane area of 130 cm^2. The experimental set-up included with a 0.5 mm sealing gasket, a peristaltic pump (Master-

flex I/P 77600-62), a valve on the retentate outlet pipe to control the transmembrane pressure (TMP), two temperature sensors, two electronic pressure sensors (Scheneider Electric XMLP) and two analogue pressure gauges placed at the module inlet and outlet on the retentate side to monitor the TMP. The feed solution was maintained at 30°C with a controlled warming plate. The cross-flow velocity was 1 ms^{-1}. The permeate was weighted continuously using an electronic balance (Radwag WLC 6/A2), to measure the permeate flow. All the data were collected with Labview software.

2.4.3. Critical pressure measurement

2 L of real or model solution were filtered and the retentate and the permeate recycled to the feed tank in order to maintain the initial feed concentration (full recycling mode). The experiments were performed at a constant temperature of 30°C, and a constant cross-flow velocity of 1 ms^{-1}.The TMP was raised from 0.2 bar (minimum pressure obtained with the retentate valve completely open), in 0.05 to 0.1 bar steps (depending on the experiment), to a maximum pressure P_{max} at which permeate fluxes do not increase any further. TMP increments were carried out only after permeate flux stabilisation at each pressure. The critical pressure P_C, above which the fouling becomes significant, was evaluated from graphs of J=f(TMP). It corresponded to the pressure above which the slope of J=f(TMP) decreased. The pressure used for concentration P_{conc} was chosen as $\leq P_C$. The experiments were per-

formed in duplicate for model solutions with all the membranes except for the PAN membrane, which was performed in triplicate. One experiment was performed with each real supernatant.

2.4.4. Concentration of the lipid fraction

2 L of solution (model solution or real supernatant) were filtered in batch mode at 30°C with the crossflow filtration set-up described above, with a cross flow velocity of 1 ms^{-1}. In all cases P_{conc} was determined following the protocol described in section 2.4.3. The used TMP (between 0.2 and 0.4 bar) is described in table 2 for model solutions and in section 3.3 for microalgae extracts. The retentate was recycled to the feed tank but the permeate was extracted. The volume reduction ratio (VRR = $\frac{V_{feed}}{V_{retentate}}$) reached 1.5 to 4 depending on the experiment. Permeate and retentate samples were collected at VRR 1.5, 2, 3, 4 according to the experiment, in order to determine pH, conductivity, dry matter, ash and droplet size distribution, and to quantify lipids, proteins, and polysaccharides. The experiments were performed in duplicate for model solutions with all the membranes except for the PAN membrane which was performed in triplicate. One experiment was performed with each real supernatant.

2.4.5. Membrane cleaning

Before and after filtration, the membranes were cleaned at 40°C following several steps: water rinsing, a cleaning step, water rinsing and if necessary bleach cleaning before strong water rinsing. The cleaning step was carried out

following two protocols: i) in the case of model solution filtration, a sodium dodecyl sulfate solution was used followed by rinsing with water/ethanol to get rid of the surfactants, and ii) in the case of real microalgae extracts filtration, a basic commercial product, Ultrasil 110 (Ecolab) was employed. Water permeability was measured before and after cleaning to determine the fouling resistances.

The filtration performances were evaluated by measuring J and the calculation of $\frac{J}{J_w}$ (equation 1) and $\%\, Flux\ decline$ (equation 2). The cleanability was evaluated by calculating the resistance of the membrane and reversible and irreversible fouling, using equation 3. Evaluation of membrane selectivity was based on the retention rate R of the different compounds, calculated using equation 4 and/or equation 5 .

$$\frac{J}{J_w} = \frac{\frac{TMP}{\mu(R_m+R_f)}}{\frac{TMP}{\mu R_m}} = \frac{R_m}{R_m + R_f} \tag{1}$$

$$\%\, Flux\ decline = \frac{J_w - J}{J_w}.100 \tag{2}$$

$$J = \frac{TMP}{\mu(R_m + R_f)} = \frac{TMP}{\mu(R_m + R_{irr} + R_{rev})} \tag{3}$$

$$\ln \frac{C_R}{C_0} = R \ln VRR \tag{4}$$

$$R = 1 - \frac{C_P}{C_R} \tag{5}$$

Where J is the permeate flux during the filtration of the emulsion ($m^3\ m^{-2}\ s^{-1}$), J_w is the permeate flux during the filtration of clean water ($m^3\ m^{-2}\ s^{-1}$), TMP is the transmembrane pressure (Pa), μ is the permeate viscosity (Pa s), R_m is the membrane resistance (m^{-1}), R_f is the fouling resistance (m^{-1}), R_{irr} is the irreversible fouling resistance (m^{-1}), R_{rev} is the reversible fouling resistance (m^{-1}), C_0 is the concentration in the feed (g L^{-1}), C_R is the concentration in the retentate (g L^{-1}), C_P is the concentration in the permeate (g L^{-1}), R is the retention rate (-), and VRR is the volume reduction ratio (-).

2.5. Analytical methods

2.5.1. Granulometry

The droplet size distribution measurement for model solutions was performed using an optical microscope Axio Scope A1 (Carl Zeiss) with a detection limit of 0.5 μm and image analysis using the software Image J software. Between 30 to 50 photos were taken and analyzed for each sample to guarantee a number of droplets higher than 5000 and an invariable droplet diameter average. Droplet size distribution with real products was performed using a Mastersizer 3000 (Malvern) with a refractive index of 1.44 and an absorption index of 0.003, using hydro LV and hydro SV samplers.

2.5.2. Gravimetry

Dry matter was measured at 105°C up to constant weight using a moisture analyzer (Denver Instrument IR-30), which has an integrated scale with a precision of 1 mg and a readability of results of 0.01%. A 5 g sample of retentate and a 20 g sample of permeate were placed in an aluminum weighing cup prior to drying at 105°C. The ash content was measured after calcination in an oven at 500°C. Analyses were performed in triplicate.

2.5.3. Chemical analysis

The lipids in microalgae extracts were quantified using a modified Bligh Dyer method, for which a mixture of $CHCl_3$/MeOH 2:1 v/v was mixed for 6h with the biomass. Extraction was followed by solvent drying, transmethylation and GC-FID analysis for total fatty acids quantification. The detailed protocol has been described by Clavijo Rivera et al. [29]. Proteins were quantified using the Thermo Scientific Pierce BCA protein assay kit. Carbohydrates were quantified using the Dubois method [46]. The chemical analyses, for each sample, were performed in triplicate.

2.5.4. Contact angle measurement

A tensiometer Drop Shape Analyzer - DSA30 (Kruss) was used to measure the wettability of the clean membranes. The contact angle θ_w , indicating the hydrophilic ($\theta_w \leq 90°$) or hydrophobic ($\theta_w \geq 90°$) characteristics of the membrane, was determined as follows. Membranes were dried at 35°C for 24h and cooled for 24h in a desiccator. The membranes were fixed to

a glass support using tape. A 2.5μL drop was placed on the surface of the membrane using automatic drop dosing and a syringe of 500μL. The DSA software was used to determine the left and right angles formed between the drop and the membrane surface at 100 ms after drop deposition. 12 droplets of water were deposited on different sections of the same membrane sample, increasing the accuracy of the average value of the contact angle (see table 1).

3. Results and discussion

3.1. Model solution formulation

The comparison of high–pressure liquid chromatography (HPLC) profiles of triglycerides from the vegetable oils mixture and the real microalgae extracts is presented in figure 1. The analysis shows a good concordance of the triglycerides of both products with some differences in proportion. This vegetable oil mixture was used to formulate the model solution. The lipid phase should have the same sensitivity to temperature and therfore the same viscoelasticity properties as microalgae lipids. This point could not be verified because the analysis would necessitate too great a quantity of real products. The droplet size distribution for the model solution obtained with laser granulometry is presented in figure 2. The distribution is bimodal, the first mode corresponding to droplets with a median diameter Dv50 of 0.07 μm and the second with a median diameter of 1.94 μm. This bimodal distribution showed similar droplet sizes to real extracts from high–pressure

disrupted microalgae despite their different proportions [29]. Depending on the composition and size distribution of the lipid droplets, the emulsion is an appropriate model for the lipids contained in concentrated aqueous extracts of *Parachlorella kessleri* cultivated in starving conditions.

3.2. Membrane selection

3.2.1. Critical pressure

The critical pressure P_C was evaluated during filtration of the model emulsion in a full recycling mode. The permeation flux J was measured against transmembrane pressure TMP and compared to the clean water flux J_w. Figure 3 illustrates the impact of the pressure on the permeation flux for the 500 kDa PAN membrane. The 500 kDa PAN membrane showed the highest material homogeneity during the conditioning and compaction stages and the least variability between experiments. As the minimum pressure for the experiment set-up was 0.2 bar, it was not possible to measure permeate fluxes at pressures below this value. $J < J_w$ due to concentration polarisation and membrane fouling. The experimental curve enabled determination of the P_C above which strong fouling takes place. For the 500 kDa PAN membrane, $P_C = 0.3$ bar.

Critical pressure values for the different membranes are shown in table 2. Despite the different membrane materials and molecular weight cut-offs (MWCO), the critical pressure was between 0.2 and 0.3 bar and the

critical fluxes between 15 and 25 L h^{-1} m^{-2}. The pressure selected to carry out concentration of the emulsion (P_{conc}) was $\leq P_C$ and is presented in table 2.

The critical pressures measured and therefore the pressures selected are similar to those selected by Giorno et al. [43] and the critical fluxes are of the same magnitude as previous studies [25; 43].

3.2.2. Emulsion filtration

Concentration of the emulsion was performed with a TMP equal to P_{conc}. The objective was to evaluate and compare the performances (permeate flux, lipid retention, and membrane cleanability) of the different membranes in the context of lipids concentration.

Permeation fluxes through the membranes against time are presented in figure 4. The flux is related to the resistance of the membrane, and the reversible and irreversible fouling using equation 3. The ratios J/J_w are also presented to illustrate the impact of the evolution of fouling resistance on the permeate flux (equation 1). Flux declines were calculated using equation 2 (table 3).

Both PVDF membranes presented the highest initial flux but also the highest flux decline at VRR=2 (volume reduction ratio) (see table 3), 80% for PVDF 0.4 µm, and 97% for PVDF 1.5 µm. This result is related to pore diameter. The flux with the membrane PVDF 0.4 µm decreased pro-

gressively, which may be due to progressive pore blocking by droplets with a diameter below the cut-off. The strong decline in permeate flux with the membrane PVDF 1.5 µm for the first hour may be due to the accumulation of larger lipid droplets above the membrane and also in the porous media. The PVDF membranes present hydrophobic properties which may facilitate interaction with the lipid fraction on the surface and at depth. These results are consistent with former papers: Lorente et al. [25] also rejected the membrane with a high MWCO for filtration and Safi et al. [24] noted strong fouling for the membranes with the highest MWCO. The PAN 500 kDa and the PES 200 kDa have smaller pores than the above membranes; this is why the initial fluxes are smaller, but more stable. PAN and PES are more hydrophilic than PVDF (*cf.* the smaller $\theta_w < 90$ in table 1). The PAN membrane presents the smallest flux decline (42%) at VRR=2, with the PES 200 kDa being the second smallest (63% at VRR=2). The slow evolution of the J/J_w ratio shows the slow evolution of the resistance due to membrane fouling.

The lipid concentrations in the retentate (C_R) and the permeate (C_P) were compared to the feed (C_0) and retention rates R deduced from equation 4.

The highest retention rates 0.95 were reached with the PAN and PES membranes, and the lowest with the PVDF 0.4 µm and PVDF 1.5 µm, respectively 0.92 and 0.87. A turbide permeate was noted with the PVDF 1.5 µm. These results can be explained by comparing the feed droplet size

distribution (figure 2) to the membranes MWCO. A large quantity of the lipid droplets are of a diameter smaller than 0.4 and 1.5 µm corresponding to the PVDF membranes.

The PVDF membranes showed low performance for the concentration of the lipids, but may be useful for making the droplets coalesce. The droplet size distribution for droplets above 0.5 µm was measured and the median diameter Dv50 during concentration compared to the initial Dv50 of the emulsion using optical microscopy (figure 5). A small rise in mean diameter was observed, but contrary to our assumption the hydrophilic membrane PAN led to the highest diameter rise during filtration. The droplets concentrate near the membrane but their limited interaction with the hydrophilic membrane may promote interaction with each other leading to coalescence. A higher VRR would lead to a higher C_R which could facilitate coalescence, but this would necessitate a larger feed volume and filtration time or a larger membrane area with a limited dead volume, which is not possible with the current experimental set-up.

Cleanability was evaluated by calculating the resistance to water permeation due to reversible (before chemical cleaning) and irreversible fouling (after chemical cleaning). The membrane showing the lowest fouling resistance was the PAN 500 kDa (table 4). The 1.5 µm PVDF showed the strongest reversible fouling and the 0.4 µm PVDF the highest irreversible fouling.

Membrane selection: the future development of membrane filtration for

the recovery of lipids at industrial scale will necessitate high and stable fluxes, a good lipid retention and high cleanability. After comparing membranes performances, the PAN 500 kDa membrane was selected as the most suitable for lipid concentration from real microalgae extracts.

3.3. Microalgae extracts filtration

Two *Parachlorella kessleri* cultures at 1g L^{-1} were used to produce two batches of clarified supernatant for filtration tests at pilot scale (SN_1 and SN_2, see part 2.2). The supernatants were filtered using the crossflow filtration set-up equipped with a PAN 500 kDa membrane. The composition of the supernatants is described in table 5. Their dry matter is 10 times less concentrated than the model solution which was chosen to simulate highly concentrated mixtures. The lipid content is also lower, corresponding to 8-12% of the dry matter. The large volume cultures were less rich in lipids than previous ones [29]. The pH and conductivity are of the same order of magnitude as the ones in the model solution. The difference in the composition was expected. The supernatant composition was impacted by the culture, the bead milling and the centrifugation conditions. Some variation of the starving condition cultures and the non optimized clarification protocole may explain the low lipid content in SN_1 and SN_2. The one-pass bead milling in experiment 2 also explains the lower protein concentrations in SN_2 compared to SN_1. 5000L of culture would have been necessary to perform a filtration leading to the same lipid content as the model solution, which

was not possible in this study. The lower concentration of the supernatants allowed a higher transmembrane pressure of 0.4 bar to be used (the critical pressure was estimated at 0.45 bar with SN_1 and SN_2). In the following paragraphs the PAN membrane performances for filtration of the real products in concentration mode are compared to the filtration with the model solution.

The fluxes are presented in table 6 and figure 6. The experiments were performed with different TMP and initial water fluxes of the membrane pieces (widespread in membrane filtration at laboratory scale). Thus the $\frac{J}{J_w}$ ratio was used for comparison. In figure 6 (a), one representative example of emulsion filtration is compared to SN_1 and SN_2 filtrations. In figure 6 (b), mean values based on three emulsion filtration experiments are compared to SN_1 and SN_2 filtrations. $\frac{J}{J_w}$ values were very similar for the filtrations using emulsion and real supernatants, maintained at between 0.38 and 0.75. Strong fouling seems to occur at the early stage of the real–products filtration (first hour) but stabilizes after 2 hours. This may be due to lipids but also to other organic compounds (proteins or polysaccharides), which are known to be common foulants. According to the results with the concentrated model solution, we can suppose that the performances would be maintained during concentration. In laboratory conditions, the maximum volume reduction ratio which could be achieved was 4. Good cleanability was also noted despite the more complicated composition of the real solution: in both experiments the irreversible fouling resistance was between 6 and 16% of the global fouling resistance (table 7), the same order of magnitude as the model solution

fouling resistance. The PAN membrane is thus very interesting for filtering supernatant with stable fluxes at various concentrations when selecting the appropriate TMP.

It might be interesting to investigate the interactions between lipids, proteins, polysaccharides and the membrane. The filtration of more complex model solutions containing proteins would help in understanding the role of the interactions on the process performances. According to Wang et al. [47] some of the proteins are linked to the lipid droplets. It is known that the destabilization of such emulsions into separate lipids and proteins is difficult [48]. Lipids, proteins and polysaccharides are also able to create strong membrane fouling, and specific analytical methods are needed to characterize them [49; 50]. These interactions influence the filtration performances, all the more when the concentration rises. This point should be thoroughly studied in a future work.

The flux and the ratio $\frac{J}{J_w}$ in this work are higher than those presented by Lorente et al. [25] and Safi et al. [24] (the water permeability of the PES 300 kDa membrane used by Safi et al. [24] was considered the same as the PES 200 kDa used in this work). The differences can be explained by the different clarification of the filtered product: the cell fragments may generate a strong fouling. Hawever, the choice of the membrane type and the operating conditions is also crucial. Filtration at a TMP far above the

critical pressure, as may be the case for Lorente et al. [25] and Safi et al. [24], leads to higher membrane fouling. The resistance of the irreversible fouling calculated from Lorente et al. data [25] using the equation 3 was 20 to 54 $10^{12}m^{-1}$ for the best conditions, which is 100 times higher than the irreversible fouling measured in this work.

The concentrations of the different compounds in feed, retentate, and permeate after filtration are detailed in table 5. The ash represents the mineral content and is approximately half of the feed dry matter. The minerals can be linked to the organic matter or free ionic species in solution.The organic matter is mostly composed of lipids, proteins and polysaccharides. The retention of the lipids, proteins, polysaccharides, and salts (free ionic species in the aqueous phase assimilated to conductivity) was evaluated using their concentration in the retentate and permeate at VRR=2 according to equation 5. In both cases, the lipids are wholly retained (R_{lipids}=1) and the salts are seldom retained (R_{salts}=0.12 and 0.04 for SN_1 and SN_2 respectively). The retention of proteins and polysaccharides depends on the supernatant: $R_{proteins}$= 1 and 0.55, $R_{polysaccharides}$= 0.74 and 0.38 for SN_1 and SN_2 respectively. This is probably due to the differences in the culture batch and the bead milling conditions. SN_1 comes from a strong disruption of the cells, leading to the release of many compounds (lipids and proteins, see table 5) among which some amphiphilic molecules are from the cell membranes, whereas SN_2 was produced in mild conditions. During bead milling,

a modification of the compounds may appear (hydrolysis due to the release of enzymes in the medium, polymerization or precipitation for example) or the released molecules may reorganize (new aggregates), leading to very different retentions. These results showed that protein retention is dependent on the cell disruption conditions, consistent with the results described by Safi et al. [24]. Nevertheless, the PAN membrane is likely to allow hydrophilic compounds to permeate. Optimized coupling of the processes of culture, cell disruption and filtration would allow the separation of lipids from proteins and polysaccharides. The mass balance was performed using the equation 6 to estimate wether any matter was accumulated on the membrane during the filtration.

$$V_{SN_i} C_{SN_i} = V_{RET_i} C_{RET_i} + V_{PERM_i} C_{PERM_i} + dm_i \tag{6}$$

where V is the volume and C the concentration of the different compounds, dm is the mass variation if some material is accumulated on the membrane during the filtration. 2 L of feed, 1 L of permeate and 1 L of retentate were considered at VRR = 2. The results are presented in table 5. No significant mass loss dm was calculated according to the used analytical methods and their uncertainty. The analyses were not accurate enough to estimate the mass of compounds leading to membrane fouling. The negative values for sugar were due to the analytical method uncertainty.

The granulometry measurements showed that SN_1 contained smaller par-

ticles compared to SN_2 (figure 7). Droplet size distribution also differed from the results presented by Clavijo et al. [29]. This is due to the difference in cell disruption methods. The particle or droplet distributions did not change during either of the filtration experiments. No coalescence was noticed because of the low concentration of the filtered solutions, reducing the probability of droplet collisions. Where the concentration was increased to the same magnitude as in the model solution (i.e. at a higher VRR), coalescence could appear.

4. Conclusions

This work proposes membrane cross-flow filtration for the recovery of lipids from starving *Parachlorella kessleri* aqueous extracts obtained after milling and centrifugation. Selection of the appropriate membrane for the lipids concentration necessitates a mixture with a controlled composition, so a model solution was formulated. The composition was based on the analysis of real products. The use of this model solution allowed selection of a PAN 500 kDa membrane for filtering real microalgae extracts. The PAN membrane gave the best performance in terms of flux, lipid retention and cleanability. Despite the differences in composition between real aqueous extracts and the model solution, permeation flux through the PAN membrane was similar (34 - 41 L h^{-1} m^{-2}). The lipids were wholly retained whereas some of the hydrophilic compounds were able to permeate. The results show

the high potential of cross-flow filtration in a microalgae biorefinering for the recovery of oil, as well as the importance of the membrane selection and operating conditions to boost the droplets coalescence. Additional studies using model solutions with different compositions would be useful to establish the effect of the composition on filtration performance. Further studies on a larger scale with higher VRR using real solutions with a higher lipid content are needed to determine the optimal operating conditions for oil droplet coalescence. Additionally, coupling between culture, cell disruption, clarification and filtration should allow a good concentration of lipids and the appropriate separation of lipids and hydrophilic compounds in microalgae biorefineries.

Acknowledgments. to be added after the double-blind review

Declaration of interest: none.

References

[1] L. Xu, D. W. F. Brilman, J. A. M. Withag, G. Brem, S. Kersten, Assessment of a dry and a wet route for the production of biofuels from microalgae: Energy balance analysis, Bioresource Technology 102 (8) (2011) 5113–5122. doi:http://dx.doi.org/10.1016/j.biortech.2011.01.066.
URL http://www.sciencedirect.com/science/article/pii/S0960852411001386

[2] M. Mubarak, A. Shaija, T. V. Suchithra, A review on the extraction

of lipid from microalgae for biodiesel production, Algal Research 7 (0) (2015) 117–123. doi:http://dx.doi.org/10.1016/j.algal.2014.10.008.
URL http://www.sciencedirect.com/science/article/pii/S2211926414001088

[3] R. Halim, T. W. T. Rupasinghe, D. L. Tull, P. A. Webley, Modelling the kinetics of lipid extraction from wet microalgal concentrate: A novel perspective on a classical process, Chemical Engineering Journal 242 (0) (2014) 234–253. doi:http://dx.doi.org/10.1016/j.cej.2013.12.070.
URL http://www.sciencedirect.com/science/article/pii/S1385894713016513

[4] J.-Y. Park, M. S. Park, Y.-C. Lee, J.-W. Yang, Advances in direct transesterification of algal oils from wet biomass, Bioresource Technology 184 (0) (2015) 267–275. doi:http://dx.doi.org/10.1016/j.biortech.2014.10.089.
URL http://www.sciencedirect.com/science/article/pii/S0960852414015211

[5] S. Dickinson, M. Mientus, D. Frey, A. Amini-Hajibashi, S. Ozturk, F. Shaikh, D. Sengupta, M. M. El-Halwagi, A review of biodiesel production from microalgae, Clean Technologies and Environmental Policy

19 (3) (2017) 637–668. doi:10.1007/s10098-016-1309-6.
URL https://doi.org/10.1007/s10098-016-1309-6

[6] D. Chiaramonti, M. Prussi, M. Buffi, A. M. Rizzo, L. Pari, Review and experimental study on pyrolysis and hydrothermal liquefaction of microalgae for biofuel production, Applied Energy 185 (2017) 963–972. doi:10.1016/j.apenergy.2015.12.001.

[7] Y. Su, K. Song, P. Zhang, Y. Su, J. Cheng, X. Chen, Progress of microalgae biofuel's commercialization, Renewable and Sustainable Energy Reviews 74 (2017) 402–411. doi:https://doi.org/10.1016/j.rser.2016.12.078.
URL http://www.sciencedirect.com/science/article/pii/S1364032116311352

[8] S. Khanra, M. Mondal, G. Halder, O. N. Tiwari, K. Gayen, T. K. Bhowmick, Downstream processing of microalgae for pigments, protein and carbohydrate in industrial application: A review, Food and Bioproducts Processingdoi:https://doi.org/10.1016/j.fbp.2018.02.002.
URL http://www.sciencedirect.com/science/article/pii/S0960308518300105

[9] G. P. Lam, M. H. Vermuë, M. H. M. Eppink, R. H. Wijffels, C. van den Berg, Multi-product microalgae biorefineries: From concept

towards reality, Trends in Biotechnology 36 (2) (2018) 216–227. doi:https://doi.org/10.1016/j.tibtech.2017.10.011.
URL http://www.sciencedirect.com/science/article/pii/S0167779917302755

[10] G. F. Ferreira, L. F. Ríos Pinto, R. Maciel Filho, L. V. Fregolente, A review on lipid production from microalgae: Association between cultivation using waste streams and fatty acid profiles, Renewable and Sustainable Energy Reviews 109 (2019) 448–466. doi:https://doi.org/10.1016/j.rser.2019.04.052.
URL http://www.sciencedirect.com/science/article/pii/S1364032119302643

[11] M. L. Menegazzo, G. G. Fonseca, Biomass recovery and lipid extraction processes for microalgae biofuels production: A review, Renewable and Sustainable Energy Reviews 107 (2019) 87–107. doi:https://doi.org/10.1016/j.rser.2019.01.064.
URL http://www.sciencedirect.com/science/article/pii/S1364032119300577

[12] P. Jaouen, L. Vandanjon, F. Quemeneur, The shear stress of microalgal cell suspensions (tetraselmis suecica) in tangential flow filtration systems: the role of pumps, Bioresource Technology 68 (2) (1999) 149–154. doi:10.1016/s0960-8524(98)00144-8.
URL <GotoISI>://WOS:000078343200006

[13] M. Frappart, A. Masse, M. Y. Jaffrin, J. Pruvost, P. Jaouen, Influence of hydrodynamics in tangential and dynamic ultrafiltration systems for microalgae separation, Desalination 265 (1-3) (2011) 279–283. doi:10.1016/j.desal.2010.07.061.
URL <GotoISI>://WOS:000285449800039

[14] S. D. Rios, J. Salvado, X. Farriol, C. Torras, Antifouling microfiltration strategies to harvest microalgae for biofuel, Bioresource Technology 119 (2012) 406–418. doi:10.1016/j.biortech.2012.05.044.
URL <GotoISI>://WOS:000307617600052

[15] M. R. Bilad, V. Discart, D. Vandamme, I. Foubert, K. Muylaert, I. F. Vankelecom, Coupled cultivation and pre-harvesting of microalgae in a membrane photobioreactor (mpbr), Bioresour Technol 155 (2014) 410–7. doi:10.1016/j.biortech.2013.05.026.
URL http://www.ncbi.nlm.nih.gov/pubmed/24559585

[16] M. L. Gerardo, S. Van Den Hende, H. Vervaeren, T. Coward, S. C. Skill, Harvesting of microalgae within a biorefinery approach: A review of the developments and case studies from pilot-plants, Algal Research 11 (2015) 248–262. doi:10.1016/j.algal.2015.06.019.

[17] F. Zhao, H. Chu, X. Tan, Y. Zhang, L. Yang, X. Zhou, J. Zhao, Comparison of axial vibration membrane and submerged aeration membrane in microalgae harvesting, Bioresour Technol 208 (2016) 178–183.

doi:10.1016/j.biortech.2016.02.099.
URL https://www.ncbi.nlm.nih.gov/pubmed/26943935

[18] F. Fasaei, J. H. Bitter, P. M. Slegers, A. J. B. van Boxtel, Techno-economic evaluation of microalgae harvesting and dewatering systems, Algal Research 31 (2018) 347–362. doi:10.1016/j.algal.2017.11.038.

[19] N. Rossignol, P. Jaouen, J.-M. Robert, F. Quéméneur, Production of exocellular pigment by the marine diatom haslea ostrearia simonsen in a photobioreactor equipped with immersed ultrafiltration membranes, Bioresource Technology 73 (2) (2000) 197–200. doi:https://doi.org/10.1016/S0960-8524(99)00171-6.
URL http://www.sciencedirect.com/science/article/pii/S0960852499001716

[20] M. L. Gerardo, D. L. Oatley-Radcliffe, R. W. Lovitt, Integration of membrane technology in microalgae biorefineries, Journal of Membrane Science 464 (2014) 86–99. doi:https://doi.org/10.1016/j.memsci.2014.04.010.

[21] A. Marcati, A. V. Ursu, C. Laroche, N. Soanen, L. Marchal, S. Jubeau, G. Djelveh, P. Michaud, Extraction and fractionation of polysaccharides and b-phycoerythrin from the microalga porphyridium cruentum by membrane technology, Algal Research 5 (0) (2014) 258–263.

doi:http://dx.doi.org/10.1016/j.algal.2014.03.006.
URL http://www.sciencedirect.com/science/article/pii/S2211926414000307

[22] A.-V. Ursu, A. Marcati, T. Sayd, V. Sante-Lhoutellier, G. Djelveh, P. Michaud, Extraction, fractionation and functional properties of proteins from the microalgae chlorella vulgaris, Bioresource Technology 157 (0) (2014) 134–139. doi:http://dx.doi.org/10.1016/j.biortech.2014.01.071.
URL http://www.sciencedirect.com/science/article/pii/S0960852414000960

[23] V. Montalescot, R. Touchard, M. Frappart, J. Pruvost, P. Jaouen, P. Bourseau, Potential of membrane fractionation of wet microalgal biomass: metabolites recovery after cell disruption, in: 10th European Congress of Chemical Engineering – ECCE10, 2015.

[24] C. Safi, G. Olivieri, R. P. Campos, N. Engelen-Smit, W. J. Mulder, L. A. M. van den Broek, L. Sijtsma, Biorefinery of microalgal soluble proteins by sequential processing and membrane filtration, Bioresour Technol 225 (2017) 151–158. doi:10.1016/j.biortech.2016.11.068.
URL https://www.ncbi.nlm.nih.gov/pubmed/27888732

[25] E. Lorente, M. Haponska, E. Clavero, C. Torras, J. Salvadó, Microalgae fractionation using steam explosion, dynamic and tangential cross-flow

membrane filtration, Bioresource Technology 237 (2017) 3–10. doi:10.1016/j.biortech.2017.03.129.

[26] R. Balti, R. Le Balc'h, N. Brodu, M. Gilbert, B. Le Gouic, S. Le Gall, C. Sinquin, A. Massé, Concentration and purification of porphyridium cruentum exopolysaccharides by membrane filtration at various cross-flow velocities, Process Biochemistry 74 (2018) 175–184. doi:https://doi.org/10.1016/j.procbio.2018.06.021.
URL http://www.sciencedirect.com/science/article/pii/S1359511318304847

[27] R. Halim, B. Gladman, M. K. Danquah, P. A. Webley, Oil extraction from microalgae for biodiesel production, Bioresource Technology 102 (1) (2011) 178–185. doi:http://dx.doi.org/10.1016/j.biortech.2010.06.136.
URL http://www.sciencedirect.com/science/article/pii/S0960852410011399

[28] W. J. Bjornsson, K. M. MacDougall, J. E. Melanson, S. J. B. O'Leary, P. J. McGinn, Pilot-scale supercritical carbon dioxide extractions for the recovery of triacylglycerols from microalgae: a practical tool for algal biofuels research, Journal of Applied Phycology 24 (3) (2012) 547–555. doi:10.1007/s10811-011-9756-2.
URL <GotoISI>://WOS:000304187100030

[29] E. Clavijo Rivera, V. Montalescot, M. Viau, D. Drouin, P. Bourseau,

M. Frappart, C. Monteux, E. Couallier, Mechanical cell disruption of parachlorella kessleri microalgae: Impact on lipid fraction composition, Bioresour Technol 256 (2018) 77–85. doi:10.1016/j.biortech.2018.01.148.
URL https://www.ncbi.nlm.nih.gov/pubmed/29433049

[30] J. B. Snape, M. Nakajima, Processing of agricultural fats and oils using membrane technology, Journal of Food Engineering 30 (1996) 1–41.

[31] M. Cheryan, N. Rajagopalan, Membrane processing of oily streams . wastewater treatment and waste reduction 151.

[32] J. M. Dickhout, J. Moreno, P. M. Biesheuvel, L. Boels, R. G. H. Lammertink, W. M. de Vos, Produced water treatment by membranes: A review from a colloidal perspective, Journal of Colloid and Interface Science 487 (2017) 523–534. doi:https://doi.org/10.1016/j.jcis.2016.10.013.
URL http://www.sciencedirect.com/science/article/pii/S0021979716307652

[33] P. Kajitvichyanukul, Y.-T. Hung, L. K. Wang, Membrane Technologies for Oil–Water Separation, Vol. 13: Membrane and desalination technologies, 2011, pp. 639–668. doi:10.1007/978-1-59745-278-6_15.

[34] M. Hlavacek, Break-up of oil-in-water emulsions induced by permeation through a microfiltration membrane 102 (1995) 1–7.

[35] U. Daiminger, W. Nitsch, P. Plucinski, S. Hoffmann, Novel techniques for oil-water separation, Journal of Membrane Science 99 (2) (1995) 197–203. doi:10.1016/0376-7388(94)00218-n.
URL <GotoISI>://WOS:A1995QM53300009

[36] A. Koltuniewicz, R. Field, T. Arnot, Cross-flow and dead-end microfiltration of oily-water emulsion. part i: Experimental study and analysis of flux decline, Journal of Membrane Science 102 (1995) 193–207.

[37] Y. Hu, J. Dai, Hydrophobic aggregation of alumina in surfactant solution, Minerals Engineering 16 (11) (2003) 1167–1172. doi:10.1016/j.mineng.2003.07.018.

[38] L. Susan, S. Ismail, B. Ooi, H. Mustapa, Surface morphology of pvdf membrane and its fouling phenomenon by crude oil emulsion, Journal of water process engineering 15 (2017) 55–61.

[39] N. Scharnagl, H. Buschatz, Polyacrylonitrile (pan) membranes for ultra- and microfiltration, Desalination 139 (1) (2001) 191–198. doi:https://doi.org/10.1016/S0011-9164(01)00310-1.
URL http://www.sciencedirect.com/science/article/pii/S0011916401003101

[40] N. N. Li, A. G. Fane, W. Winston Ho, T. Matsuura, Advanced Membrane Technology and Applications, Wiley, 2008.

[41] Y. Peng, F. Guo, Q. Wen, F. Yang, Z. Guo, A novel polyacrylonitrile membrane with a high flux for emulsified oil/water separation, Separation and Purification Technology 184 (2017) 72–78. doi:10.1016/j.seppur.2017.04.036.

[42] A. Hong, A. G. Fane, R. Burford, Factors affecting membrane coalescence of stable oil-in-water emulsions, Journal of Membrane Science 222 (1-2) (2003) 19–39. doi:10.1016/s0376-7388(03)00137-6.

[43] F. Giorno, R. Mazzei, L. Giorno, Purification of triacylglycerols for biodiesel production from nannochloropsis microalgae by membrane technology, Bioresource Technology 140 (0) (2013) 172–178. doi:http://dx.doi.org/10.1016/j.biortech.2013.04.073.
URL http://www.sciencedirect.com/science/article/pii/S0960852413006962

[44] V. Montalescot, T. Rinaldi, R. Touchard, S. Jubeau, M. Frappart, P. Jaouen, P. Bourseau, L. Marchal, Optimization of bead milling parameters for the cell disruption of microalgae: Process modeling and application to porphyridium cruentum and nannochloropsis oculata, Bioresource Technology 196 (2015) 339–346. doi:https://doi.org/10.1016/j.biortech.2015.07.075.

[45] T. R. Zinkone, I. Gifuni, L. Lavenant, J. Pruvost, L. Marchal, Bead milling disruption kinetics of microalgae: Process modeling, optimiza-

tion and application to biomolecules recovery from chlorella sorokiniana, Bioresour Technol 267 (2018) 458–465. doi:10.1016/j.biortech.2018.07.080.
URL https://doi.org/10.1016/j.biortech.2018.07.080

[46] M. Dubois, K. A. Gilles, Colorimetric method for determination of sugars and related substances, Analytical Chemistry.

[47] X. Wang, T.-B. Hao, S. Balamurugan, W.-D. Yang, J.-S. Liu, H.-P. Dong, H.-Y. Li, A lipid droplet-associated protein involved in lipid droplet biogenesis and triacylglycerol accumulation in the oleaginous microalga phaeodactylum tricornutum, Algal Research 26 (2017) 215–224. doi:10.1016/j.algal.2017.07.028.

[48] R. Morales Chabrand, H.-J. Kim, C. Zhang, C. E. Glatz, S. Jung, Destabilization of the emulsion formed during aqueous extraction of soybean oil, Journal of the American Oil Chemists' Society 85 (4) (2008) 383–390. doi:10.1007/s11746-008-1199-9.

[49] D. Delaunay, M. Rabiller-Baudry, J. M. Gozálvez-Zafrilla, B. Balannec, M. Frappart, L. Paugam, Mapping of protein fouling by ftir-atr as experimental tool to study membrane fouling and fluid velocity profile in various geometries and validation by cfd simulation, Chem. Eng. Process. 47 (7) (2008) 1106 – 1117, euromembrane 2006. doi:10.1016/j.cep.2007.12.008.

URL http://www.sciencedirect.com/science/article/pii/S025527010700390X

[50] V. Drevet, E. Clavijo, L. Villafaña López, M. Frappart, E. Couallier, A. Szymczyk, M. Rabiller Baudry, Characterisation of the fouling of an ultrafiltration polyethersulfone membrane fouled by an emulsion modelling lipids issued from microalgae, in: ICOM, 2017.

List of Figures

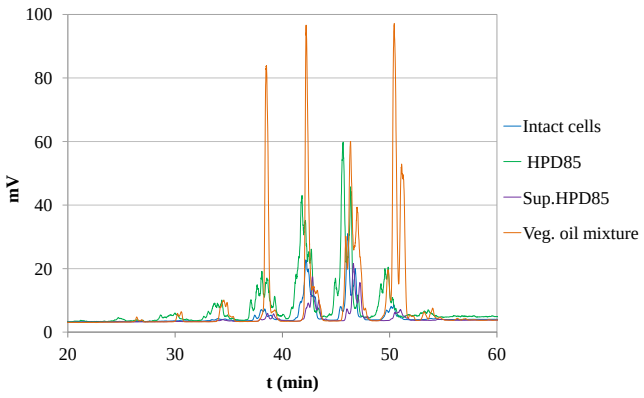

Figure 1 – Comparison of triglycerides profiles from the vegetable oils mixture and intact *Parachlorella kessleri* cells, ground cells (High Pressure Disruption 85%, HPD85) and supernatant (Sup.HPD85) after centrifugation.

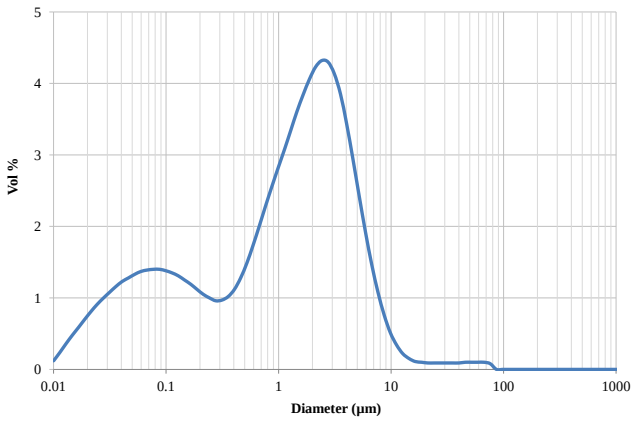

Figure 2 – Droplet size distribution (volume) of the initial emulsion before filtration obtained with laser granulometry.

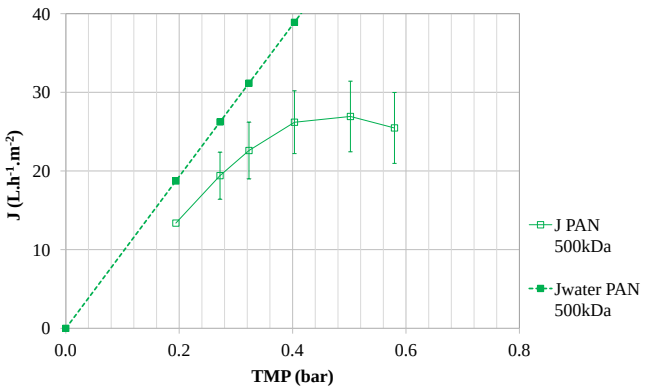

Figure 3 – Filtration of the model emulsion with a PAN 500 kDa membrane in full recycling mode (constant temperature 30°C, constant cross-flow velocity 1 ms^{-1}) to determine critical pressure: measurement of flux J versus transmembrane pressure TMP with water (filled squares) and with the model solution (empty square).

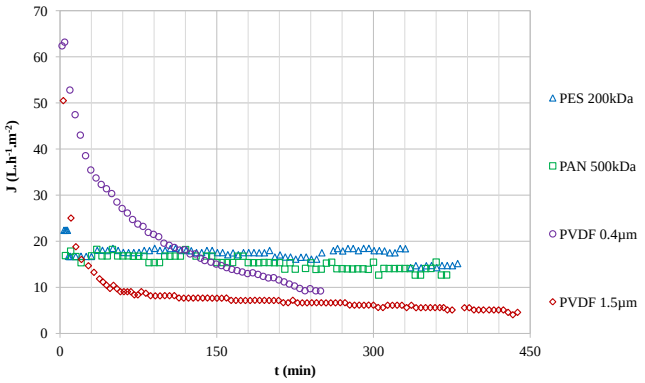

(a)

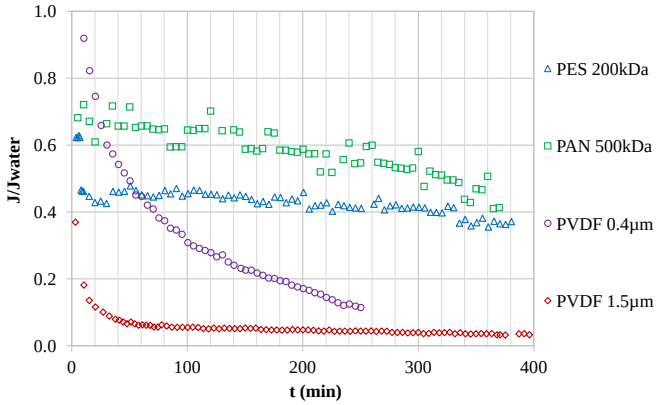

(b)

Figure 4 – Filtration of the model emulsion in concentration mode with the different membranes: (a) flux J and (b) ratio J/J_w versus time (constant temperature 30°C, constant cross-flow velocity 1 ms^{-1}, PTM = 0.2 bar).

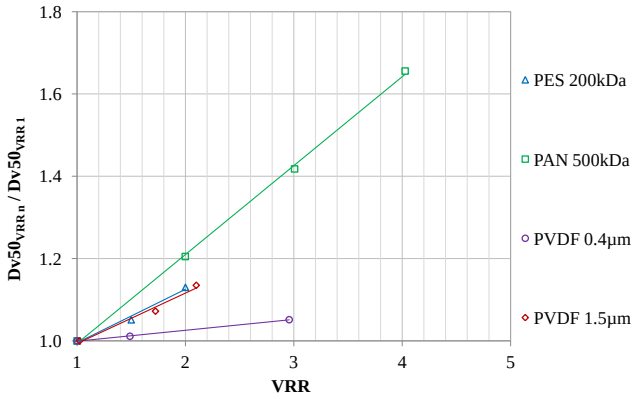

Figure 5 – Evolution of the Dv50 for droplets with a diameter above 0.5 µm during the concentration of model emulsion versus the volume reduction ratio for different membranes.

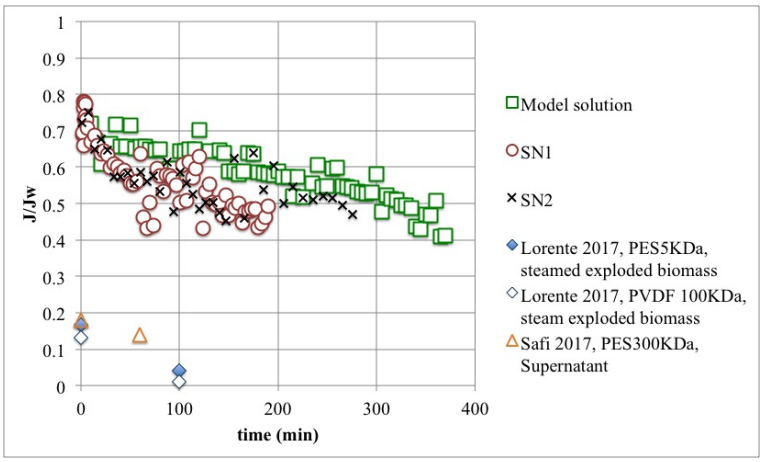

(a)

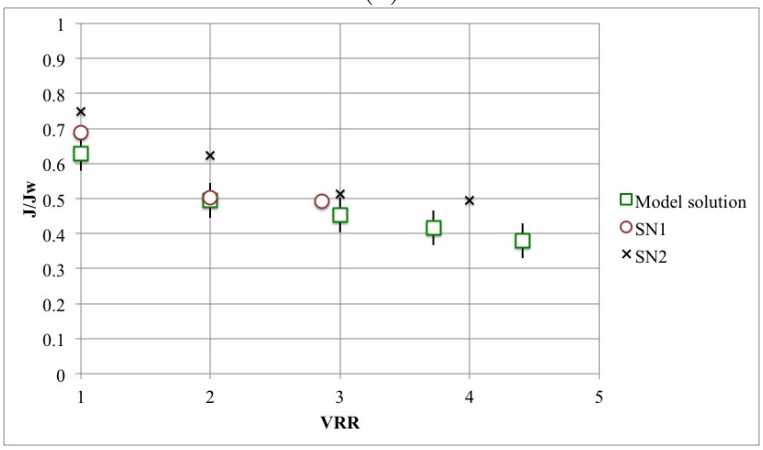

(b)

Figure 6 – Comparison of crossflow filtrations of the model solution and the two supernatants SN_1 and SN_2 in concentration mode with a PAN 500 kDa membrane. Constant temperature 30°C, constant cross-flow velocity 1 ms^{-1}. The TMP was 0.2 bar for the model solution, 0.4 bar for SN_1 and SN_2 : ratio J/J_w versus time (a) and VRR (b). Comparison with the results from Lorente et al. [25] and Safi et al. [24] (TMP = 5 bar for Lorente et al. [25] and 2.07 bar for Safi et al. [24])

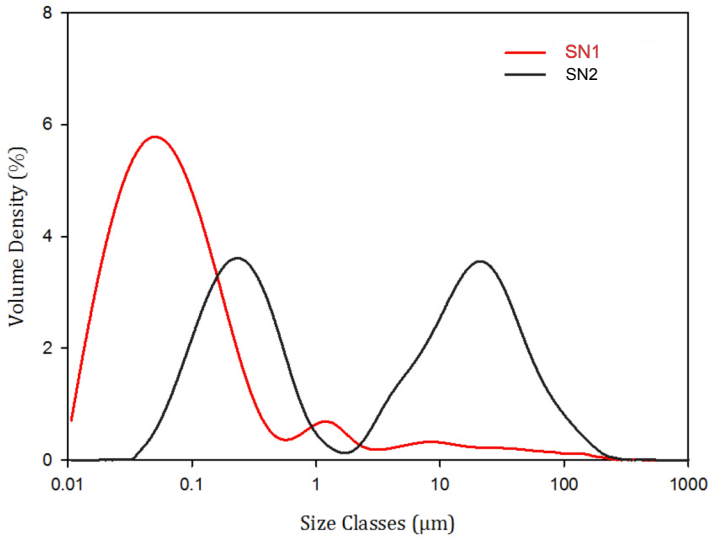

Figure 7 – Droplet size distribution (volume) for supernatants SN_1 and SN_2 before filtration obtained with laser granulometry.

List of Tables

Table 1 – Characteristics of the membranes used in this study. Molar weight cut-off (MWCO), contact angle (θ_w).

Polymer	MWCO	Classification	θ_w (°)
PES	200 kDa	UF	79.4 ± 0.5
PAN	500 kDa	UF	75.0 ± 2.4
PVDF	0.4 µm	MF	95.1 ± 1.2
PVDF	1.5 µm	MF	82.3 ± 0.7

Table 2 – Critical Pressure P_C, critical flux J_C, maximum pressure P_{max} and maximum flux J_{max} measured during filtration of the model emulsion in full recycling mode on the different membranes and pressure selected for the concentration step P_{conc}.

Polymer	MWCO	P_C (bar)	J_C (L h^{-1} m^{-2})	P_{max} (bar)	J_{max} (L h^{-1} m^{-2})	P_{conc} (bar)
PES	200 kDa	0.3	25 ± 15	0.4	25 ± 15	0.2
PAN	500 kDa	0.3	17 ± 5	0.4	20 ± 5	0.2
PVDF	0.4 µm	0.2	15 ± 5	0.2	15 ± 5	0.2
PVDF	1.5 µm	0.2	25 ± 10	0.3	28 ± 7	0.2

Table 3 – Water flux J_w (L h^{-1} m^{-2}) measured at P_{conc}, permeate flux J (L h^{-1} m^{-2}) at VRR = 2 measured during filtration of the model emulsion at the concentration step, and flux decline (%) at VRR = 2 for the different membranes.

Polymer	cut off	J_w	J	$\%\, Flux\ decline$
PES	200 kDa	40	15	63
PAN	500 kDa	26	15	42
PVDF	0.4 µm	80	16	80
PVDF	1.5 µm	163	4	97

Table 4 – Resistance (x10^{12} m^{-1}) to the permeation flow due to the membrane media (R_m), reversible fouling(R_{rev}) and irreversible fouling (R_{irr}), leading to a total resistance R_{tot} during filtration of the model solution with four different membranes.

Polymer	cut off	R_m	R_{rev}	R_{irr}	R_{tot}
PES	200 kDa	2.9	4.0	0.8	7.7
PAN	500 kDa	1.4	2.2	0.2	3.7
PVDF	0.4 µm	1.4	3.1	5.1	9.6
PVDF	1.5 µm	0.7	26	0.1	26.8

Table 5 – Composition of the supernatants SN_1 and SN_2 of bead-milled *Parachlorella kessleri* cultures before filtration and composition of the retentates and permeates sampled at volume reduction ratio VRR=2 for both filtration experiments. DM: Dry matter (g L^{-1}). Cond.: conductivity (µS cm^{-1}). Lipids, proteins, sugar, ash: in g L^{-1}. *dm* the mass variation (g) if some material accumulated on the membrane during the filtration (estimated through mass balance).

	SN_1	RET1	PERM1	*dm* 1	SN_2	RET2	PERM2	*dm* 2
DM	2.0 ±0.1	2.8	1.1	0.1 ±0.2	1.4 ±0.1	1.6	1	0.2 ±0.2
Lipids	0.16 ±0.02	0.29	0	0.03 ±0.04	0.17 ±0.02	0.3	0	0.04 ±0.04
Proteins	0.38 ±0.05	0.60	0	0.16 ±0.1	0.19 ±0.03	0.27	0.12	0.01 ±0.06
Sugar	0.45 ±0.04	0.95	0.25	-0.3 ±0.08	0.32 ±0.07	0.50	0.23	-0.09 ±0.08
Ash	1.05 ±0.1				0.95 ±0.25			
Cond.	1049 ±8	1211	1024		993 ±20	1004	969	
pH	7.60	7.9	8.1		7.2	7.3	7.5	

Table 6 – Comparison of the fluxes (L h^{-1} m^{-2}) and permeabilities (L h^{-1} m^{-2} bar^{-1}) obtained during filtration of SN_1 and SN_2 with a PAN membrane at 0.4bar (Several membrane pieces were used, presenting a variation of water permeability before filtration, due to material non homogeneity).

	SN_1	SN_2
Water flux J_w	72	95
Water permeability L_w	180	237
Initial flux J_i	52	70
Initial permeability L_i	130	175
Flux(VRR=2) $J_{VRR=2}$	34	41
Permeability (VRR=2) $L_{VRR=2}$	84	103

Table 7 – Resistance to the permeation flow ($10^{12}m^{-1}$) due to the membrane media (R_m), reversible fouling(R_{rev}) and irreversible fouling (R_{irr}), leading to a total resistance R_{tot} during the filtration of the model solution, SN_1 and SN_2 with the PAN membrane.

filtered solution	R_m	R_{rev}	R_{irr}	R_{tot}
model solution	1.4	2.2	0.15	3.7
SN_1	2	1.9	0.37	4.3
SN_2	1.5	1.8	0.13	3.5